

pubs.acs.org/NanoLett Letter

Programming the Curvatures in Reconfigurable DNA Domino Origami by Using Asymmetric Units

Dongfang Wang, Lei Yu, Bin Ji, Shuai Chang,* Jie Song,* and Yonggang Ke*



Cite This: https://dx.doi.org/10.1021/acs.nanolett.0c03348



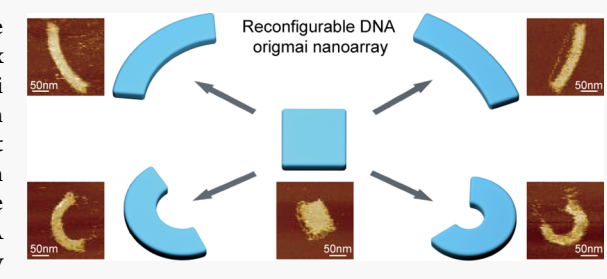
ACCESS

Metrics & More

Article Recommendations

Supporting Information

ABSTRACT: The DNA origami technique is a robust method for the design of DNA nanostructures with prescribed shapes, including complex curved geometries. In addition to static structures, dynamic DNA origami has been used to construct sophisticated nanomachines that can reconfigure their shapes in response to external stimuli. Here, we report a new method to design DNA origami structures that can transform between a noncurved conformation and curved conformation. The reconfigurable structures are developed on the basis of dynamic DNA domino origami, which can transform in a cascading process initiated by trigger DNA strands. The degree of curvature could be programmed by tuning the sizes of DNA units within the origami.



KEYWORDS: DNA domino origami, dynamic DNA origami, conformation transformation, curved conformation

he programmable self-assembly of DNA has enabled the construction of 1D, 1-3 2D, 4-12 and 3D structures. 13-20 Importantly, the invention of the DNA origami technique, 11 in which a long single-stranded DNA scaffold is folded to customdesigned shapes via hybridization with hundreds of short DNA strands, dramatically facilitates the design of complex DNA structures. Many interesting DNA structures with tailored features have been designed using DNA origami and employed in various applications. 21-27 DNA origami can be used to construct not only nanostructures consisting of straight DNA helices but also curved objects formed by bent DNA helices. Currently, there are three general methods to design curved DNA structures. The first one is to design noncurved DNA origami and then generate curvatures by using deletions and insertions of base pairs in the DNA structures.²⁸ The second one is to arrange the DNA scaffold based on the geometry of a curved design and then generate corresponding DNA staples subsequently.²⁹ The third one is to bend the DNA helices by mechanical tension. 30,31

In addition to static DNA origami, many dynamic DNA origami nanostructures have been developed, such as hinges, 32 switches, 33 walkers, 34 and rotary devices. 35 Recently, it has been demonstrated that DNA origami can undergo conformation change by shifting the base stacking at the junctions, including transformation induced by external mechanical force in DNA origami tubes, 36 and a cascade reaction in a DNA domino array triggered by the DNA trigger strands. 37,38 Here, we demonstrate that a new dynamic DNA origami domino array can be used as a general platform for generating tunable curvatures in DNA origami nanostructures. The programmable DNA domino array is formed by connecting many small dynamic DNA units and can transform between two stable

conformations in a step-by-step cascading process initiated by the addition of trigger DNA strands (Figure 1A). The canonical domino arrays do not contain engineered curvatures, before or after transformation. In this work, we adjust the sizes of DNA units to introduce a "unit size gradient" in the DNA domino array and show that the curvature in a DNA domino array can be controlled by adjusting the unit size gradient.

Design. The reconfigurable curved DNA origami is adapted from the reconfigurable DNA domino array in a previous publication.³⁷ In the reconfigurable DNA origami array, the DNA origami is composed of interconnected small dynamic DNA units. A unit contains four DNA duplex domains with equal length and four dynamic nicking points, which act as hinges. The unit can switch between two stable conformations, through the intermediate conformation. The transformation of an individual unit in the presence of trigger DNA strands can propagate to its neighbor units and eventually leads to global structural transformation. In the canonical DNA domino array, each DNA unit has the same size. The DNA helices in both conformations have the same lengths, so both conformations of the DNA structure are noncurved (Figure 1A). In the new design, a DNA domino array consists of a gradient in terms of the sizes of DNA units (Figure 1B). Before transformation, the domino array retains a rectangular shape, because all DNA

Received: August 17, 2020 Revised: October 13, 2020



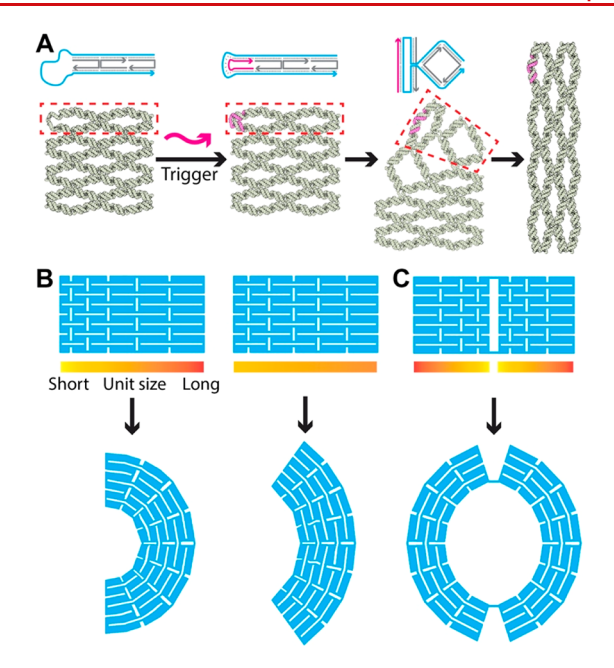


Figure 1. Schematic of reconfigurable domino origami arrays with programmable curvatures. (A) A canonical four-by-three DNA domino array is formed by interconnected dynamic DNA antijunction units with uniform size. An array can switch between two stable conformations with the help of trigger DNA strands. Strand diagrams show the interactions between DNA strands corresponding to structures in the red boxes. In the canonical design, both conformations of DNA origami are noncurved. (B) In a DNA domino array with a gradient distribution of unit sizes, the array can switch between a noncurved rectangular conformation and a curved conformation. In the rectangular conformation, the DNA helices have equal lengths. In the curved conformation, the DNA helices have different lengths, which lead to tunable curvatures. (C) The design concept can be used to realize more complex transformation between noncurved structures and curved structures. For example, a two-part rectangle can transform to a ring-shaped structure. In addition, each part of the structure can be transformed independently.

helices have equal lengths, regardless of the unit size gradients. However, after transformation initiated by trigger DNA strands, the directions of DNA helices reoriented, and the array now contains DNA helices with different lengths, which cause the DNA domino array to display a predesigned curvature to compensate the local stress. The degree of curvatures in the curved conformation can be tuned with the unit size gradients. We also demonstrate more complex transformations by using tube-shaped structures and DNA domino arrays containing multiple parts that can be independently transformed into curved shapes (Figure 1C).

Results. We designed four different two-dimensional DNA origami arrays with the same overall dimensions but varied unit size gradients (see Figure S1 for design schematics; see Figures S23–S26 for the design diagram). The staple DNA strands were classified into core strands, helper strands, and trigger strands. Trigger strands were used for the transformation and to stabilize the curved conformation, while the helper strands can stabilize the rectangular conformation. The four arrays were designed to exhibit various degrees of continuous curvatures after transformation from rectangle shapes to curved shapes (see Figure S2 for the schematics of four curved conformations). To characterize the two conformations of each DNA domino array, we assembled each of the four structures with one-pot annealing using a p7560 DNA scaffold.

The four domino arrays were designed to have the same dimensions but different unit size gradients (Figure 2A). Before transformation, AFM imaging revealed that the rectangular conformation (V1R, V2R, V3R, V4R) assembled with core strands shared similar dimensions (Figure 2A and Figure S3). After being converted to the curved transformations, the curved domino arrays (V1C, V2C, V3C, V4C) exhibited a varied degree of curvatures, in accordance with their unit size gradients. The curvature of each version was measured by calculating the central angles the structures in AFM images (see Figure S3 for details). The central angles for versions 1-4 were $44.3^{\circ} \pm 0.9^{\circ}$ (N = 50), $78.3^{\circ} \pm 1.3^{\circ}$ (N = 67), $174.1^{\circ} \pm 1.2^{\circ}$ (N = 84), and $232.9^{\circ} \pm 1.9^{\circ}$ (N = 56), respectively (Figure 2B). The central angles were consistent with the unit size gradients in the structures. With the steeper unit size gradient, the central angle becomes bigger. The native agarose gel electrophoresis further revealed the band mobilities of the different conformations of the four structures without purification (Figure S4). The curved conformations migrated slower than the rectangular conformations for versions 2-4 because the curved geometries reduced the migration speed in the agarose gel. However, the version 1 curved conformation migrated faster than the rectangular conformation, likely due to its relatively low level of curvature.

We investigated the transformation further by carefully studying the conditions for the transformation with agarose gel electrophoresis and AFM imaging (Figures S5 and S6). The domino origami transformation can be accelerated by adding denaturation reagent formamide ^{39,40} or incubation at higher temperatures.³⁶ After screening different conditions, we chose to add the trigger strands to the rectangular conformation samples, incubated with 20% formamide at different temperatures to achieve the desired transformation rate. No transformation or uncompleted transformations were observed in the samples at low temperatures of 30, 40, or 50 $^{\circ}$ C, while most of the rectangular conformation could be transformed into the curved conformation completely with the addition of trigger strands with the 20% formamide and 55°C incubation within 3 h (Figure 2A, Figures S6 and S7). Real-time AFM was employed to study the in situ single-molecule transformation using the version 1 structure (Figure 2C and Figure S8). We observed multiple transformations from the rectangular conformation to curved conformation within the 15 min scan. Most of the transformations started from a corner and propagated through a diagonal pathway. A few transformations initiated from two corners and propagated from two opposite directions. The *in situ* imaging revealed that the transformation was a multistep process. It initiated from a starting point by the trigger strands and propagated to the neighboring units and finally to the entire structure. We also observed that the transformations were faster when the sample was subjected to the contact force from the AFM tip (Figure S9), a phenomenon in agreement with our previous finding.³⁷

The same as the canonical domino array, the transformation between the rectangular conformation and curved conformation in the curved domino array is reversible. We demonstrated the reverse transformation from the curved conformation to the rectangular conformation on the version 4 using toehold-carrying trigger strands, corresponding releasing strands, and reverse trigger strands. The releasing strands can displace the toehold-carrying trigger strands by toehold-mediated strand displacement. The reverse trigger strands were designed at the same position as trigger strands, but they would stabilize

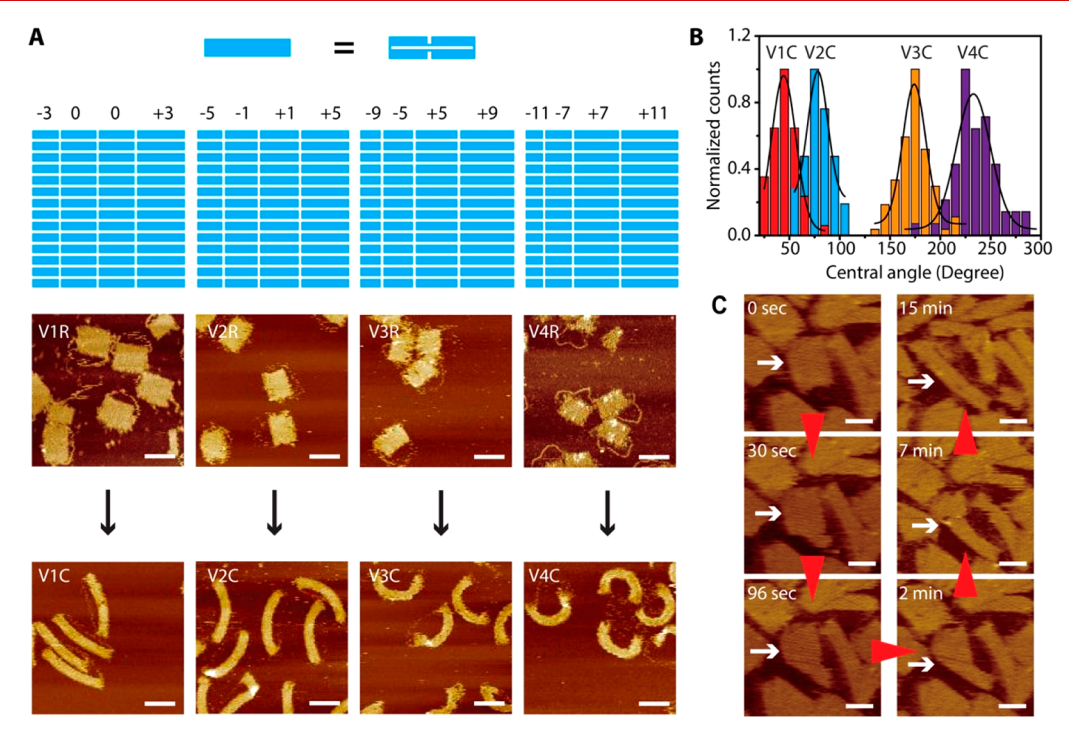


Figure 2. Transformation of rectangular conformation to curved conformation. (A) Design and transformation of four DNA domino origami arrays. The four DNA domino arrays were designed with various deletions and insertions of base pairs based on the standard 52BP antijunction unit, indicated by the numbers above each origami, to generate different unit size gradients. Each small blue rectangle represents an antijunction unit. The four rectangle-shaped DNA domino arrays (V1R–V4R) have identical dimensions before transformation. After transformation, the domino arrays displayed different curvatures (V1C–V4C) according to their unit size gradients. The steeper the gradient, the more curvature the origami exhibited. For transformation, rectangular-shaped DNA domino arrays were incubated with trigger strands and 20% formamide at 55 °C for 3 h. Each structure before or after transformed was characterized by AFM imaging. Scale bars: 100 nm. (B) Histogram of central angle distributions of the four curved DNA domino arrays. The central angles are $44.3^{\circ} \pm 1.9^{\circ}$ (N = 50), $78.3^{\circ} \pm 1.3^{\circ}$ (N = 67), $174.1^{\circ} \pm 1.2^{\circ}$ (N = 84), and $232.9^{\circ} \pm 1.9^{\circ}$ (N = 56), respectively. (C) In situ AFM imaging shows the real-time transformation of the version 1 DNA domino array from the rectangular conformation to the curved conformation in the presence of trigger strands at room temperature. The real-time transformation of one DNA origami domino array indicated by an arrow is shown. The transformation initiated at a corner and propagated to neighboring regions. Scale bars: 50 nm.

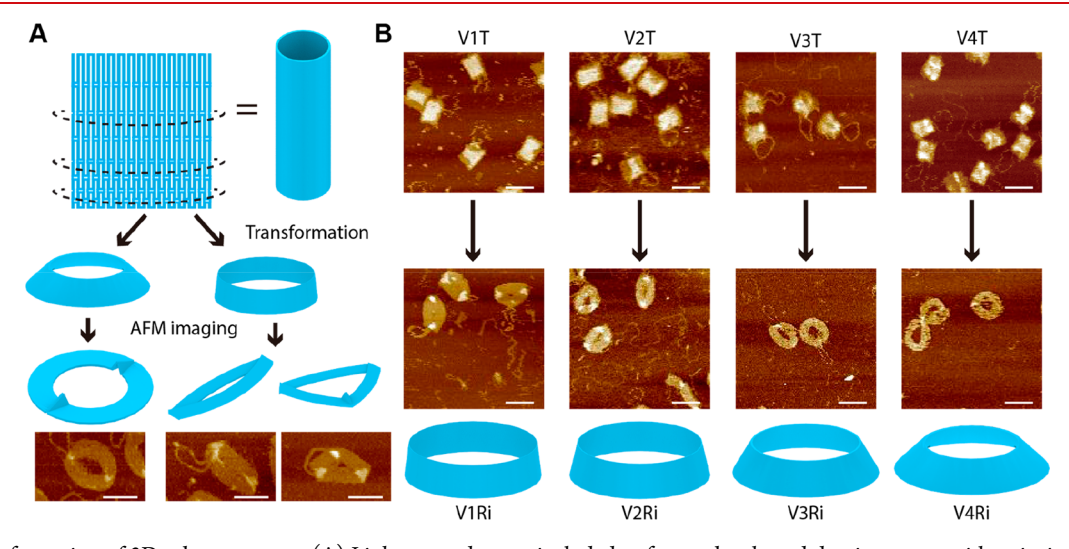


Figure 3. Transformation of 3D tube structures. (A) Linker strands were included to form tube-shaped domino arrays with unit size gradients. The tubes can transform into different ring-shaped conformations, depending on the unit size gradients. The rings were flattened on the mica surface and exhibited overlapping regions during the AFM imaging. (B) Transformation of version 1–4 tube conformations to ring conformations. Trigger strands were added to the tube samples with 20% formamide and 50 °C incubation for 2 h. Scale bars: 100 nm.

the rectangular conformation (see Figures S10 and S11 for the design details). Both AFM imaging and agarose gel electrophoresis were used to characterize the reverse transformation. Releasing the trigger strands from V4C did not revert the

curved conformation back to the rectangle conformation (Figure S11). However, adding the reverse trigger strands and 20% formamide at 40°C transformed V4C into the rectangular conformation with the yield of 29%, while increasing the

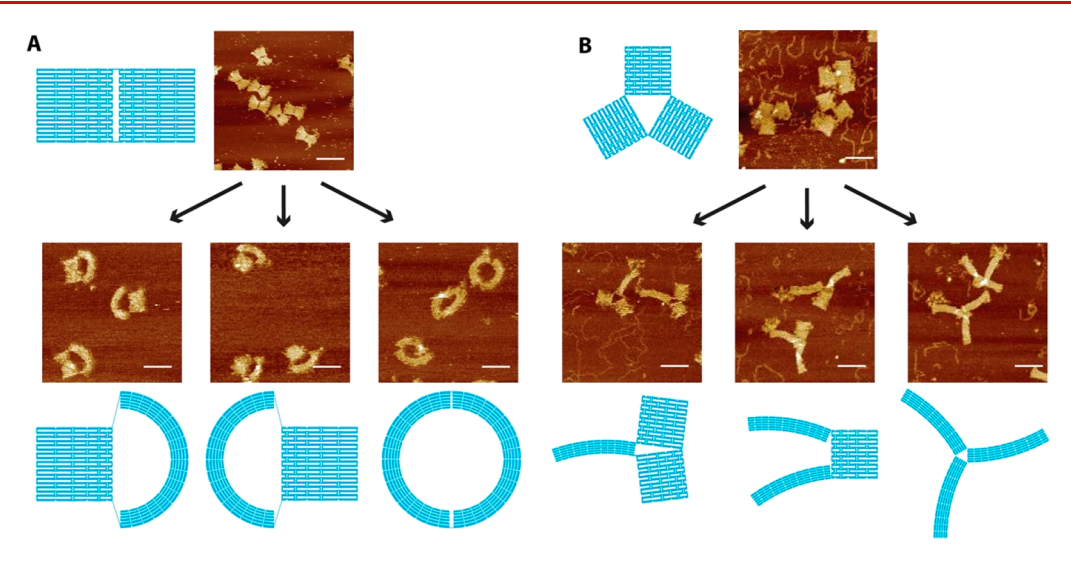


Figure 4. Modular design of curved DNA domino arrays. (A) Modular transformation from a two-part rectangular domino array to an O-shaped structure. Each part can be independently transformed to a half-circle curved structure. (B) Modular transformation from a three-part domino array to a clover-shaped structure. Each part can be selectively transformed into a curved structure. The transformation was performed by adding selective trigger strands with 20% formamide and 50 °C incubation for 2 h. Scale bars: 100 nm.

temperature to 50°C would further increase the reverse transformation yield to 100% (Figure S11).

After demonstrating the transformation from noncurved arrays to curved arrays with programmable curvatures, we expanded the curvature transformation from 2D to 3D by using tube structures. Linker strands were used to connect the edges of the version 1-4 domino arrays to form reconfigurable tubes (Figure 3A, see Figures S28-S31 for design diagram). The structures assembled with the linkers resulted in tube conformations with various unit size gradients (V1T, V2T, V3T, V4T), which were then transformed to ring conformations (V1Ri, V2Ri, V3Ri, V4Ri) with different geometries after the addition of trigger strands (Figure 3B and Figure S12). Instead of a flat two-dimensional disc, the ring conformations were three-dimensional. Thus, overlapping regions on the ring conformations were observed during the AFM imaging process, presumably because the rings were flattened on the mica surface (Figure 3A,B). The number of overlapping regions varied, depending on the specific geometries of the ring conformations. The ring conformation under AFM imaging exhibited round or eclipse shapes. The diameter of the round shape or the short axis of the eclipse shape were measured to reflect the roundness of the shapes (Figure S13).

The native agarose gel electrophoresis in Figure S4 revealed that the tube conformation migrated faster than the ring conformation in four structures, probably due to the more compact shapes of the tube conformations. The transformations were also investigated by using 20% formamide and 50 or 60 $^{\circ}$ C incubation (Figures S14—S17). We found that the tube structures could be successfully converted to ring structures in 20% formamide with 60 $^{\circ}$ C incubation (Figure 3B). We also noticed that increasing the incubation temperature to 50 or 60 $^{\circ}$ C would open a few tubes, likely due to the dehybridization of linkers.

The transformation between the tube conformation and the ring conformation was also reversible. We evaluated the reverse transformation of V4Ri to V4T by using toehold-carrying trigger strands, releasing strands, and reverse strands (Figure S10). First, the V4Ri was assembled with toehold-carrying trigger strands. Then, the trigger strands were removed from

V4Ri by adding releasing strands. Upon the addition of reverse strands, the V4Ri was transformed to V4T with \sim 100% yield with 20% formamide and 50 °C incubation (Figure S18).

We then demonstrated more complex transformations between noncurved domino arrays and curved domino arrays by designing domino arrays containing multiple interconnected but independent reconfigurable modules. Two modular domino structures were constructed. The first one is a two-part rectangle domino array that could be transformed to an Oshaped structure (Figure 4A, see Figure S33 for the design diagram). Each part of it has its own trigger strands and could be independently transformed from a rectangular conformation into a curved conformation. After successful assembly of the rectangular conformation (Figure S19), we selectively added trigger strands to transform either the left part or the right part to the curved conformation. When both parts were transformed to the curved conformation at the same time, the overall structure exhibited a ring shape as we designed (Figure 4A and Figure S20). We then designed and tested a three-part clover-shaped modular domino array (Figure 4B). The clover structure has three parts connected by the DNA scaffold (see Figure S34 for strand diagram). Like the O-shaped structure, each part in the clover-shaped structure has its independent trigger strands and can be transformed from a rectangular conformation to a curved conformation selectively. We successfully assembled the clover-shaped domino array without curvature (Figure S21) and then performed a modular transformation to curved conformations by selectively adding trigger strands (Figure 4B and Figure S22).

In summary, we demonstrated a method for the design and construction of sophisticated dynamic DNA arrays that can be controllably reconfigured between the noncurved conformation and curved conformations. The new method is fully programmable. In the dynamic DNA array consisting of interconnected DNA units, each DNA unit experiences the reconfiguration during the conformation transformation and can propagate to the neighboring units, leading to continuous curvature in the curved conformation. The curvature of the structure after transformation could be programmed by adjusting the gradient DNA unit size, generating a variety of

curved conformations from the rectangular conformation. The modular reconfiguration allows the creation of a dynamic molecular machine containing hybrid reconfigurable curved modules. Each module can independently respond to external stimuli and changes to the curved conformation. The transformation between the noncurved conformation and curved conformation expands the scope of shape changes in dynamic DNA nanostructures, allowing the creation of more sophisticated dynamic molecular machines.

ASSOCIATED CONTENT

Supporting Information

The Supporting Information is available free of charge at https://pubs.acs.org/doi/10.1021/acs.nanolett.0c03348.

Additional figures and details on materials and methods including the preparation, purification, AFM imaging of DNA origami samples, and list of all the staple strands and other DNA (PDF)

All designs in caDNAno format (ZIP)

AUTHOR INFORMATION

Corresponding Authors

- Shuai Chang The State Key Laboratory of Refractories and Metallurgy, the Institute of Advanced Materials and Nanotechnology, Wuhan University of Science and Technology, Wuhan, Hubei 430081, China; orcid.org/0000-0001-7405-5555; Email: schang23@wust.edu.cn
- Jie Song Institute of Nano Biomedicine and Engineering, Department of Instrument Science and Engineering, School of Electronic Information and Electrical Engineering, Shanghai Jiao Tong University, Shanghai 200240, China; ◎ orcid.org/0000-0002-4711-6014; Email: sjie@stju.edu.cn
- Yonggang Ke Wallace H. Coulter Department of Biomedical Engineering, Georgia Institute of Technology and Emory University, Atlanta, Georgia 30322, United States; orcid.org/0000-0003-1673-2153; Email: yonggang.ke@emory.edu

Authors

- Dongfang Wang Wallace H. Coulter Department of Biomedical Engineering, Georgia Institute of Technology and Emory University, Atlanta, Georgia 30322, United States; Institute of Nano Biomedicine and Engineering, Department of Instrument Science and Engineering, School of Electronic Information and Electrical Engineering, Shanghai Jiao Tong University, Shanghai 200240, China; ⊚ orcid.org/0000-0001-8112-3149
- Lei Yu The State Key Laboratory of Refractories and Metallurgy, the Institute of Advanced Materials and Nanotechnology, Wuhan University of Science and Technology, Wuhan, Hubei 430081, China; orcid.org/0000-0002-7107-9137
- Bin Ji Institute of Nano Biomedicine and Engineering, Department of Instrument Science and Engineering, School of Electronic Information and Electrical Engineering, Shanghai Jiao Tong University, Shanghai 200240, China

Complete contact information is available at: https://pubs.acs.org/10.1021/acs.nanolett.0c03348

Notes

The authors declare no competing financial interest.

■ ACKNOWLEDGMENTS

Y.K. acknowledges the support of the National Science Foundation under Grant DMR-1654485. J.S. acknowledges the support of the National Natural Science Foundations of China Grants 81822024, 11761141006, and 21605102 and Natural Science Foundations of Shanghai Grants 19520714100 and 19ZR1475800. The AFM images were collected on an atomic force microscope supported by Grants GM084070 and 3R01GM084070-07S1.

■ REFERENCES

- (1) Park, S. H.; Barish, R.; Li, H.; Reif, J. H.; Finkelstein, G.; et al. Three-Helix Bundle DNA Tiles Self-Assemble into 2D Lattice or 1D Templates for Silver Nanowires. *Nano Lett.* **2005**, *5*, 693–696.
- (2) Schulman, R.; Winfree, E. Synthesis of crystals with a programmable kinetic barrier to nucleation. *Proc. Natl. Acad. Sci. U. S. A.* **2007**, *104*, 15236.
- (3) Yin, P.; Hariadi, R. F.; Sahu, S.; Choi, H. M.; Park, S. H.; et al. Programming DNA tube circumferences. *Science* **2008**, 321, 824–826.
- (4) Yan, H.; Park, S. H.; Finkelstein, G.; Reif, J. H.; LaBean, T. H. DNA-Templated Self-Assembly of Protein Arrays and Highly Conductive Nanowires. *Science* **2003**, *301*, 1882–1884.
- (5) Ke, Y.; Ong, L. L.; Sun, W.; Song, J.; Dong, M.; et al. DNA Brick Crystals with Prescribed Depths. *Nat. Chem.* **2014**, *6*, 994.
- (6) Winfree, E.; Liu, F.; Wenzler, L. A.; Seeman, N. C. Design and self-assembly of two-dimensional DNA crystals. *Nature* **1998**, 394, 539–544.
- (7) Rothemund, P. W.; Papadakis, N.; Winfree, E. Algorithmic Self-Assembly of DNA Sierpinski Triangles. *PLoS Biol.* **2004**, *2*, No. e424.
- (8) He, Y.; Tian, Y.; Chen, Y.; Deng, Z.; Ribbe, A. E.; et al. Sequence symmetry as a tool for designing DNA nanostructures. *Angew. Chem., Int. Ed.* **2005**, 44, 6694–6696.
- (9) Wang, P.; Gaitanaros, S.; Lee, S.; Bathe, M.; Shih, W. M.; et al. Programming Self-Assembly of DNA Origami Honeycomb Two-Dimensional Lattices and Plasmonic Metamaterials. *J. Am. Chem. Soc.* 2016, 138, 7733
- (10) Liu, W.; Halverson, J.; Tian, Y.; Tkachenko, A. V.; Gang, O. Self-Organized Architectures from Assorted DNA-Framed Nanoparticles. *Nat. Chem.* **2016**, *8*, 867.
- (11) Rothemund, P. W. Folding DNA to Create Nanoscale Shapes and Patterns. *Nature* **2006**, 440, 297.
- (12) Wei, B.; Dai, M.; Yin, P. Complex shapes self-assembled from single-stranded DNA tiles. *Nature* **2012**, 485, 623–626.
- (13) Gerling, T.; Wagenbauer, K. F.; Neuner, A. M.; Dietz, H. Dynamic DNA devices and assemblies formed by shape-complementary, non-base pairing 3D components. *Science* **2015**, 347, 1446.
- (14) Chen, J.; Seeman, N. C. Synthesis from DNA of a molecule with the connectivity of a cube. *Nature* **1991**, *350*, *631*–*633*.
- (15) Shih, W. M.; Quispe, J. D.; Joyce, G. F. 1.7-kilobase single-stranded DNA that folds into a nanoscale octahedron. *Nature* **2004**, 427, 618–621.
- (16) Goodman, R. P.; Schaap, I. A. T.; Tardin, C. F.; Erben, C. M.; Berry, R. M.; et al. Rapid Chiral Assembly of Rigid DNA Building Blocks for Molecular Nanofabrication. *Science* **2005**, *310*, 1661–1665.
- (17) He, Y.; Ye, T.; Su, M.; Zhang, C.; Ribbe, A. E.; et al. Hierarchical self-assembly of DNA into symmetric supramolecular polyhedra. *Nature* **2008**, *452*, 198–201.
- (18) Andersen, E. S.; Dong, M.; Nielsen, M. M.; Jahn, K.; Subramani, R.; et al. Self-assembly of a nanoscale DNA box with a controllable lid. *Nature* **2009**, *459*, 73–76.
- (19) Douglas, S. M.; Dietz, H.; Liedl, T.; Hogberg, B.; Graf, F.; et al. Self-assembly of DNA into nanoscale three-dimensional shapes. *Nature* **2009**, 459, 414–418.
- (20) Ke, Y.; Ong, L. L.; Shih, W. M.; Yin, P. Three-dimensional structures self-assembled from DNA bricks. *Science* **2012**, 338, 1177–1183.

- (21) Langecker, M.; Arnaut, V.; Martin, T. G.; List, J.; Renner, S.; et al. Synthetic Lipid Membrane Channels Formed by Designed DNA Nanostructures. *Science* **2012**, 338, 932.
- (22) Douglas, S. M.; Bachelet, I.; Church, G. M. A logic-gated nanorobot for targeted transport of molecular payloads. *Science* **2012**, 335, 831–834.
- (23) Douglas, S. M.; Chou, J. J.; Shih, W. M. DNA-Nanotube-Induced Alignment of Membrane Proteins for NMR Structure Determination. *Proc. Natl. Acad. Sci. U. S. A.* **2007**, *104*, 6644.
- (24) Derr, N. D.; Goodman, B. S.; Jungmann, R.; Leschziner, A. E.; Shih, W. M.; et al. Tug-of-war in motor protein ensembles revealed with a programmable DNA origami scaffold. *Science* **2012**, *338*, 662–665.
- (25) Maune, H. T.; Han, S. P.; Barish, R. D.; Bockrath, M.; Goddard, W. A.; et al. Self-Assembly of Carbon Nanotubes into Two-Dimensional Geometries Using DNA Origami Templates. *Nat. Nanotechnol.* **2010**, *5*, 61.
- (26) Sun, W.; Boulais, E.; Hakobyan, Y.; Wang, W. L.; Guan, A.; et al. Casting inorganic structures with DNA molds. *Science* **2014**, 346, 1258361.
- (27) Nickels, P. C.; Wunsch, B.; Holzmeister, P.; Bae, W.; Kneer, L. M.; et al. Molecular force spectroscopy with a DNA origami-based nanoscopic force clamp. *Science* **2016**, *354*, 305–307.
- (28) Dietz, H.; Douglas, S. M.; Shih, W. M. Folding DNA into twisted and curved nanoscale shapes. *Science* **2009**, 325, 725–730.
- (29) Han, D.; Pal, S.; Nangreave, J.; Deng, Z.; Liu, Y.; et al. DNA origami with complex curvatures in three-dimensional space. *Science* **2011**, 332, 342–346.
- (30) Liedl, T.; Högberg, B.; Tytell, J.; Ingber, D. E.; Shih, W. M. Self-Assembly of Three-Dimensional Prestressed Tensegrity Structures from DNA. *Nat. Nanotechnol.* **2010**, *5*, 520.
- (31) Suzuki, Y.; Kawamata, I.; Mizuno, K.; Murata, S. Large Deformation of a DNA-Origami Nanoarm Induced by the Cumulative Actuation of Tension-Adjustable Modules. *Angew. Chem., Int. Ed.* **2020**, *59*, 6230–6234.
- (32) Marras, A. E.; Zhou, L.; Su, H. J.; Castro, C. E. Programmable Motion of DNA Origami Mechanisms. *Proc. Natl. Acad. Sci. U. S. A.* **2015**, *112*, 713.
- (33) Kuzyk, A.; Schreiber, R.; Zhang, H.; Govorov, A. O.; Liedl, T.; et al. Reconfigurable 3D plasmonic metamolecules. *Nat. Mater.* **2014**, 13, 862–866.
- (34) Wickham, S. F.; Bath, J.; Katsuda, Y.; Endo, M.; Hidaka, K.; et al. A DNA-based molecular motor that can navigate a network of tracks. *Nat. Nanotechnol.* **2012**, *7*, 169–173.
- (35) Ketterer, P.; Willner, E. M.; Dietz, H. Nanoscale Rotary Apparatus Formed from Tight-Fitting 3D DNA Components. *Sci. Adv.* **2016**, *2*, No. E1501209.
- (36) Endo, M.; Yamamoto, S.; Emura, T.; Hidaka, K.; Morone, N.; et al. Helical DNA Origami Tubular Structures with Various Sizes and Arrangements. *Angew. Chem., Int. Ed.* **2014**, *53*, 7484–7490.
- (37) Song, J.; Li, Z.; Wang, P.; Meyer, T.; Mao, C.; et al. Reconfiguration of DNA molecular arrays driven by information relay. *Science* **2017**, 357, No. eaan 3377.
- (38) Kosinski, R.; Mukhortava, A.; Pfeifer, W.; Candelli, A.; Rauch, P.; et al. Sites of high local frustration in DNA origami. *Nat. Commun.* **2019**, *10*, 1061.
- (39) Blake, R. D.; Delcourt, S. G. Thermodynamic Effects of Formamide on DNA Stability. *Nucleic Acids Res.* **1996**, 24, 2095–2103
- (40) McConaughy, B. L.; Laird, C. D.; McCarthy, B. J. Nucleic acid reassociation in formamide. *Biochemistry* **1969**, *8*, 3289–3295.
- (41) Simmel, F. C.; Yurke, B.; Singh, H. R. Principles and Applications of Nucleic Acid Strand Displacement Reactions. *Chem. Rev.* **2019**, *119*, 6326–6369.